

## Correction for pile-up effects based on pixel-by-pixel calibration for tomography with Medipix3RX detector

---

### Jean Rinkel<sup>1</sup>

*Brazilian Synchrotron Light Laboratory (LNLS/CNPEM) - Detector Group*

*Rua Giuseppe Máximo Solfaro, 10.000 - Caixa Postal 6192 - 13083-970 - Campinas/SP, Brazil*

*E-mail: jean.rinkel@lnls.br*

### Debora Magalhães

*Brazilian Synchrotron Light Laboratory (LNLS/CNPEM) - Detector Group*

*Rua Giuseppe Máximo Solfaro, 10.000 - Caixa Postal 6192 - 13083-970 - Campinas/SP, Brazil*

*E-mail: debora.magalhaes@lnls.br*

### Eduardo X. Miqueles

*Brazilian Synchrotron Light Laboratory (LNLS/CNPEM) - Image Group*

*Rua Giuseppe Máximo Solfaro, 10.000 - Caixa Postal 6192 - 13083-970 - Campinas/SP, Brazil*

*E-mail: eduardo.miqueles@lnls.br*

The dispersion of individual pixels parameters is widely studied in the field of hybrid pixel detectors for X-ray detection. CERN is developing methods of thresholds equalization to correct for threshold dispersion between pixels of the Medipix3RX readout chip. In this paper, we focus on the complex problem of pixel-to-pixel dead time dispersion, due to the dispersion of the shape of analog pulses and to the residual threshold dispersion after equalization. In tomography, dead time inhomogeneity is responsible for ring artefacts, in addition to global underestimation of the attenuation coefficients due to pile-up. While the main methods of ring artefact correction are purely mathematical, our strategy was to develop a method based on dead time calibration to be able to remove ring artefacts and at the same time to restore the correct quantitative attenuation coefficients. Our original correction method relies on the calibration of the detector dead time map associated to an iterative correction on the sinograms. We performed a fine analysis of dead time dispersion and compared it to our model of photonic noise propagation to validate the calibration step. The results of the pile-up correction with a single Medipix3RX ASIC bump bonded to 300 microns Silicon sensor showed quantitative improvements of reconstructions of samples acquired using a Siemens X-Ray tube and on the tomographic beam line of the Brazilian Synchrotron (LNLS).

*Technology and Instrumentation in Particle Physics 2014*

*2-6 June, 2014*

*Amsterdam, the Netherlands*

---

<sup>1</sup>Speaker

## 1. Introduction

Hybrid silicon photon-counting detectors can meet the requirements of very high dynamic range and high detection efficiency especially needed for tomographic applications using synchrotron radiation. Compared to other families of hybrid pixel detectors, such as Pilatus [1] and XPAD [2], the Medipix3RX readout chip enables a higher spatial resolution with a pixel size of 55  $\mu\text{m}$  by 55  $\mu\text{m}$ . Furthermore, this chip takes advantage of the 130 nm CMOS technology to allow a high level of functionality in each pixel, enabling correction of the charge diffusion in the sensor (charge summing mode) or allowing up to 8 energy thresholds per cluster of four pixels (spectroscopic mode). Unfortunately, some characteristics of analog and digital circuits of the ASICS are responsible for a non-linear relationship between measurement and incident flux. One of these characteristics, the shaping time, is directly related to the dead time of the system, which is responsible for pile up effects [3]. The pixel-to-pixel dispersion of these non-linear parameters cannot be corrected by simple flat field normalization. In tomography, these dispersions are responsible for ring artefacts, in addition to global false estimation of the reconstructed attenuation coefficients.

Some approaches [4, 5] are based on a model of sinogram corruption assuming that the deviation does not depend on the angle of view  $\theta$  but only on the pixel. In other words, the part of this deviation related to the sample inhomogeneity is not taken into account. The error term  $\varepsilon$  can be expressed as a function of the corrupted sinogram  $Att(\text{pixel}, \theta)$  and the original sinogram  $Sino(\text{pixel}, \theta)$ :

$$\varepsilon(\text{pixel}) = Sino(\text{pixel}, \theta) - Att(\text{pixel}, \theta) \quad (1)$$

We express now the original sinogram as a function of the incident count rate after crossing the sample, denoted  $N$ , and without sample  $N_0$  and the corrupted sinogram function of the measured count rate after crossing the sample, denoted  $M$ , and without sample  $M_0$ :  $Sino(\text{pixel}, \theta) = -\log(N(\text{pixel}, \theta)/N_0(\text{pixel}))$  and  $Att(\text{pixel}, \theta) = -\log(M(\text{pixel}, \theta)/M_0(\text{pixel}))$ . The error term is finally given by:

$$\varepsilon = \log\left(\frac{M_0}{N_0}\right) + \log\left(\frac{N}{M}\right) \quad (2)$$

The second term of the last equation depends on the object composition and by this way on  $\theta$ . Most nonlinear effects, as pile-up phenomenon, tend to increase with the incident flux. Indeed this term should increase with flux, deteriorating the artefact correction for low-attenuation objects with classical approaches [4, 5]. Our original method of ring artefact correction consists of a fast dead time characterization and of a pile-up correction taking into account the corruption of both variables  $M_0$  and  $M$  in equation (2). We evaluated the robustness of the proposed algorithm for ring artefact correction on measurements performed with a Medipix3RX ASIC bump bonded to 300 microns Silicon sensor used in conventional Single Pixel Mode, configured with single 24-bit counters and high gain mode [6]. Detector was readout using Medipix3 USB interfaces and Pixelman software [7] with threshold equalization based on the noise level. Performance of the proposed approach on tomographic reconstructions are compared to those

obtained by a state-of-the art approach [5] on acquisitions performed with a Siemens X-ray tube and on the imaging beam line of the Brazilian Synchrotron (LNLS).

## 2. Dead time calibration

### 2.1 Reference method

The reference method [8] is based on measurements with a conventional x-ray source. The count rates were recorded at various tube current values from 5 to 60 mA for a tube voltage of 20 kVp. The incident count rates are assumed to be proportional to the measurement with the lowest current. Using these measurements and the calculated incident count rates, we estimated the dead time per pixel by fitting the data with a paralyzable model of pile-up. The main parameter influencing the shape of the analogic pulse is the current within the preamplifier, called IKrum. This parameter has to be adjusted considering the trade-off between energy resolution and electronic noise vs dead time as summarized in Fig.1. For the experiments of this paper, it is fixed to 1.17 nA (5 DAC steps), which corresponds to the configuration with the best energy resolution and noise but highest dead time.

Fig.2 shows dead time measurements for 40 pixels and the dispersion in the detector. The dead time dispersion is mainly due to the variation of the shape of the analogic pulse driven by IKrum current and to the residual threshold dispersion after equalization. To validate our dispersion measurements, we developed a model describing the propagation of the photonic noise on dead time dispersion in the simple case of two measurements  $m_1$  and  $m_N$ ,  $N$  being the ratio between the two corresponding tube currents. Assuming  $N \gg 1$  to simplify the calculation of noise propagation, the standard deviation of dead time can be approximated by the following function of  $m_1$ ,  $m_N$  and  $N$ :

$$\sigma_{phot} = \frac{1}{N} \times \left( 1 - \log \left( \frac{N \times m_1}{m_N} \right) \right) \times m_1^{-3/2} \quad (3)$$

Fig. 3 shows a comparison between the measured dispersions and the contributions of the photonic noise evaluated by equation (3). The photonic contribution is significantly higher for the 10 s vs 40 s since it is directly related to the number of counted photons, which is not the case for the detector contribution. In conclusion, our measured dispersions are mainly due to the detector.

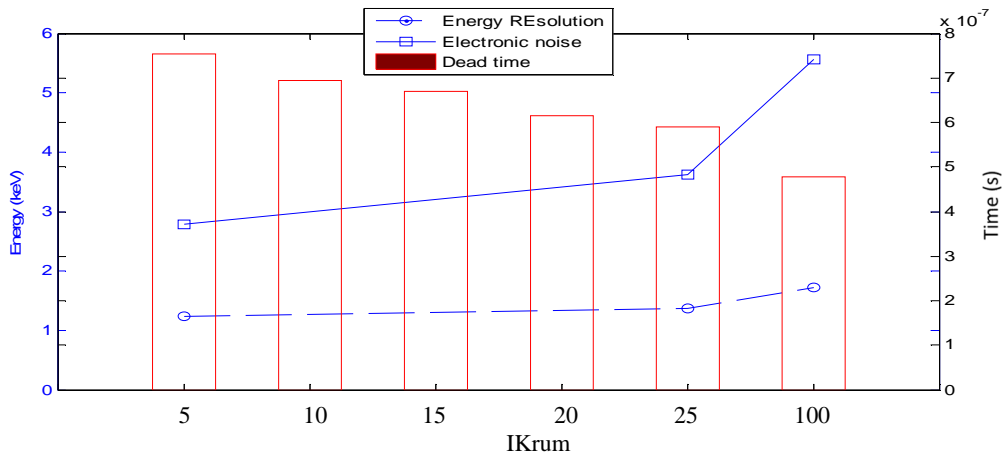


Fig.1 - Energy resolution, electronic noise and dead time function of IKrum current. Energy resolution and electronic noise are related to the left y axis (energy in keV) and dead time is related to the right y axis (time in s)

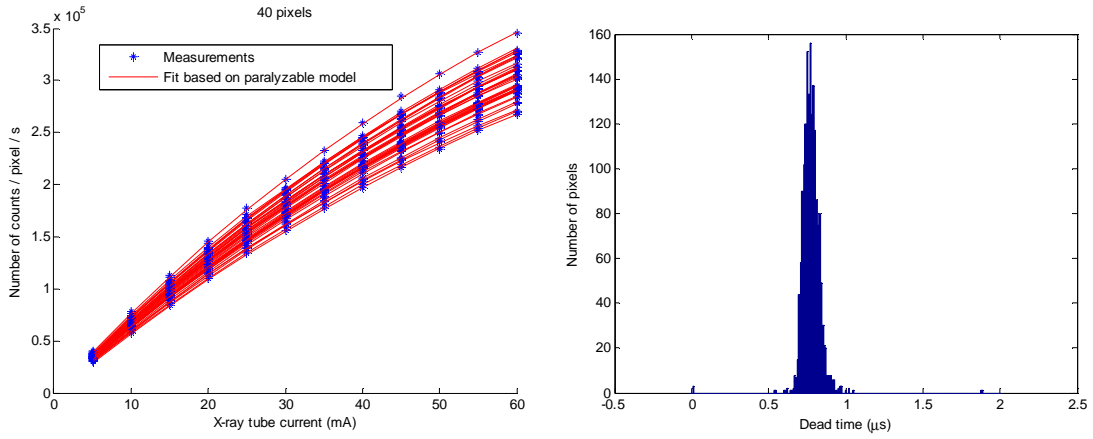


Fig.2 - Dead time measurements for 40 pixels (left) and dispersion in the detector (right)

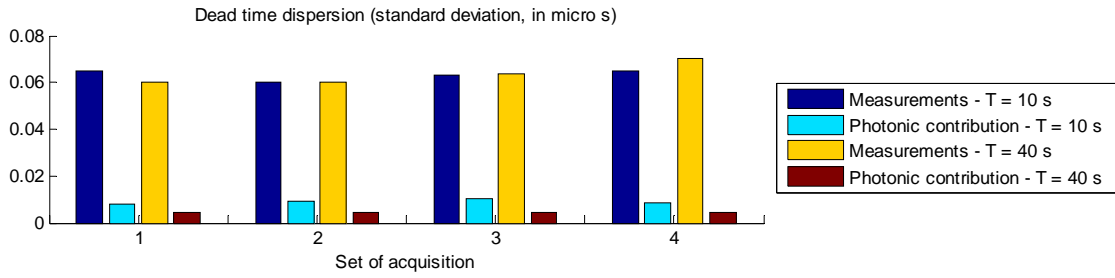


Fig.3 – Dead time dispersion for 4 different sets of acquisition using 10 s and 40 s acquisition time (T) for the lowest current measurement and contribution of the photonic noise

## 2.2 New method

For synchrotron experiments the flux has to be adjusted by filters. The reference method cannot be adapted directly because of the difficulty of knowing exactly the transmission of the filters, especially for polychromatic beams. Furthermore, the dead time has to be calibrated for each new threshold equalization, resulting in a need for a fast procedure. The new method relies on two acquisitions: the flat field ( $M_0$ ) and the radiographic image of a filter ( $M_f$ ). The image of transmission, denoted TR, is obtained by calculating the ratio pixel-per-pixel between  $M_f$  and  $M_0$ . The mean transmission over the whole image, TRmean, is then calculated. Then, the dead time variation around its mean value is calculated by first order Taylor approximation:

$$\delta\tau = (TR - TR_{mean}) \times \left(\frac{\partial TR}{\partial \tau}\right)^{-1} \quad (4)$$

In the case of a paralyzable dead time model:  $\frac{\partial TR}{\partial \tau} \approx M_0 \times TR$ , which gives:

$$\delta\tau = \frac{TR - TR_{mean}}{M_0 \times TR} \quad (5)$$

Finally, the dead time value can be calculated using an a priori knowledge of the mean dead time value  $\tau_{mean}$ :  $\tau = \tau_{mean} + \delta\tau$ . This method is illustrated in Fig.4.

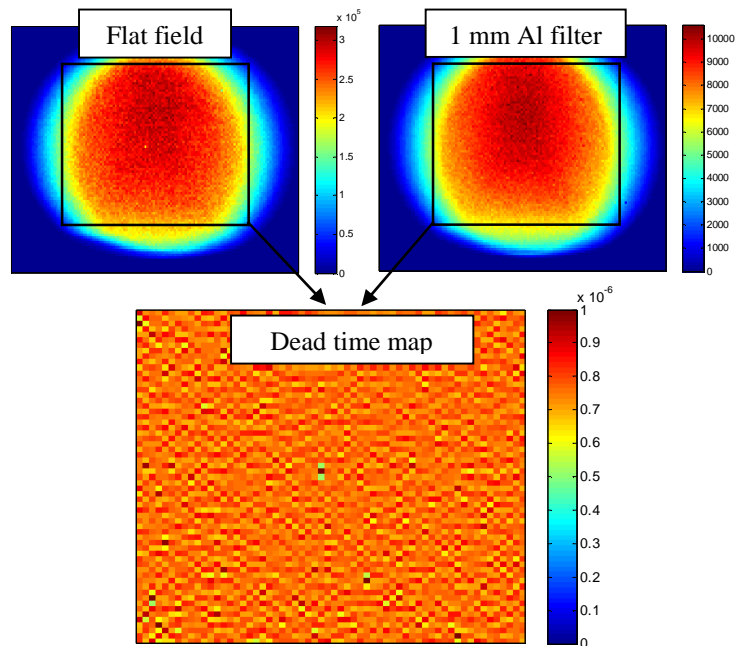


Fig. 4 – Illustration of the new procedure for fast dead time calibration

As a first validation, Fig.5 shows the comparison between the dead time histograms obtained with the new vs reference method. The robustness of the method was evaluated by varying the filter thickness, using Al filters in the range [100 – 1000]  $\mu\text{m}$  (see Fig.6).

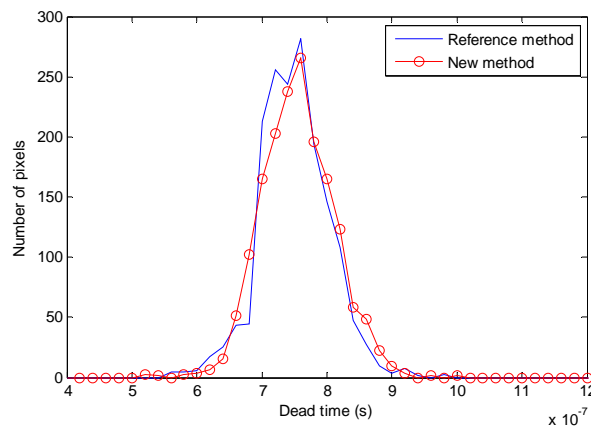


Fig. 5 – Dead time histograms calculated with the reference method and the new procedure

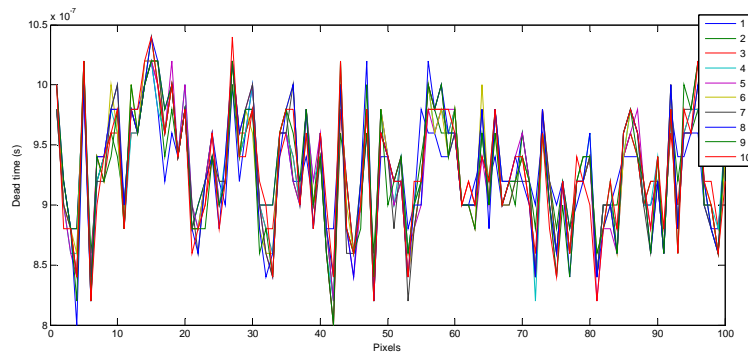


Fig. 6 – Dead time measurements of 100 pixels by the new method as a function of the Al filter thickness (100  $\mu\text{m}$  to 1000  $\mu\text{m}$  by 100- $\mu\text{m}$  step)

POS(TIPP2014)212

### 3.Pile-up correction

#### 3.1 Method

For a paralyzable pile-up model, the measurement  $M$  can be expressed as a function of incident count rates  $N$  and dead time  $\tau$ :

$$M = Ne^{-N\tau} \quad (6)$$

It is easy to observe that function  $h(N) = Ne^{-N\tau}$  attains a global maximum at the point  $N_{max} = 1/\tau$ , which implies that  $h$  is a bounded function in the interval  $0 \leq h(N) \leq h(N_{max})$ . Since  $h(N_{max}) = \frac{1}{\tau e}$ , equation (6) only makes sense with  $M$  lying in the closed interval  $\left[0, \frac{1}{\tau e}\right]$ . The correction is performed using a fixed-point approach, solving the equation

$$f(N) = N \text{ with } f(N) = N + M - Ne^{-N\tau} \text{ and } M \in \left[0, \frac{1}{\tau e}\right] \quad (7)$$

We claim that a solution for (7) exist. In fact, the function  $g(N) = f(N) - N = M - h(N)$ , satisfies:  $g(0) = M > 0$  and  $g\left(\frac{1}{\tau}\right) = M - \frac{1}{\tau e} < 0$

Since  $g$  is a one-dimensional continuous function, it follows from the mean value theorem that a fixed point  $N_F \in \left[0, \frac{1}{\tau}\right]$  must exist, such that  $g(N_F) = 0$ , i.e.,  $f(N_F) = N_F$ .

Numerically, the solution  $N_F$  is obtained through the iterative method  $f(N_k) = N_k$  in such a way that  $\lim_{k \rightarrow \infty} N_k = N_F$ , since it is easy to verify that the function  $f$  is a contraction (satisfies the Lipschitz condition). Therefore, defining the initial guess  $N_0 = M$ , we iterate in order to estimate the incident count rate at the  $k^{\text{th}}$  iteration:

$$N_k = N_{k-1} + M - N_{k-1}e^{-N_{k-1}\tau} \quad (8)$$

#### 3.2 Results

Fig. 7 shows the convergence on the sinogram of the iterative correction (3 iterations are used for further results). The corresponding sinogram was acquired on a Siemens X-ray source (20 kVp – 60 mA) with a sample made of polystyrene balls inside a glass tube (Fig. 8). Fig. 9 shows reconstructions of the polystyrene sample acquired on the Siemens X-ray source and of an adult molar tooth acquired at the Imaging beam line of the Brazilian synchrotron (polychromatic beam, mean energy: 19.9 keV). The new approach is compared to the state-of-the art approach combining first order and second order finite difference [5]. For both experiments, the non-corrected reconstructions clearly suffer from ring artefact, as the state-of-the-art correction enables good artefact reduction but creating new artefacts corresponding to pixels seeing the borders of the samples, which corresponds to the limitation analyzed in the introduction. The new method eliminates the ring artefacts without introducing new ones.

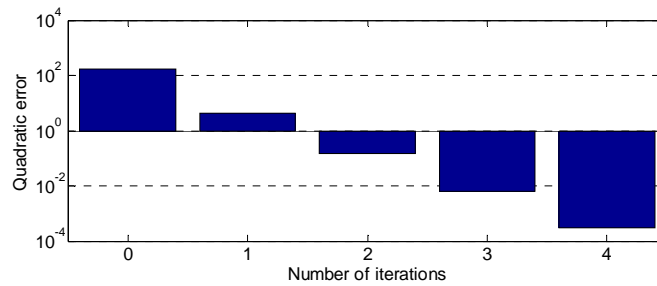


Fig. 7 – Residual quadratic error function of the number of iterations

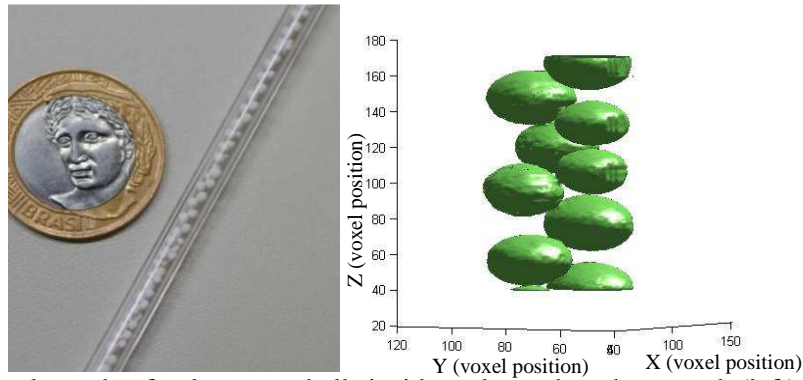


Fig. 8 – Sample made of polystyrene balls inside a glass tube: photograph (left) and 3D reconstruction (right)

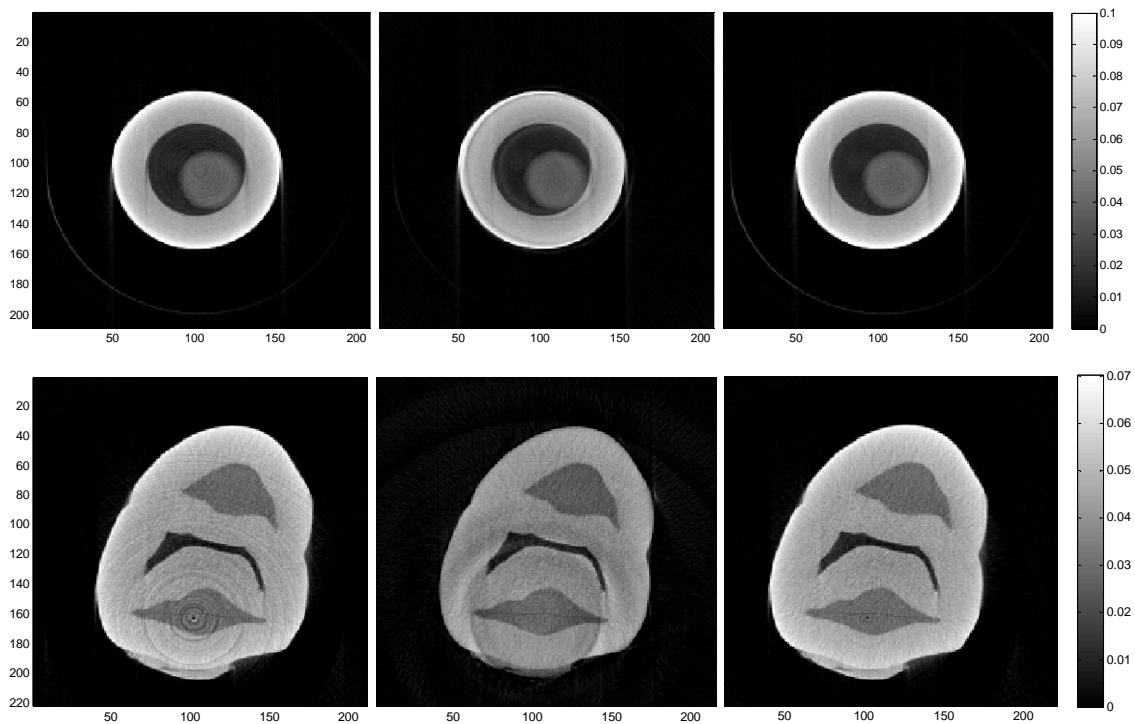


Fig. 9 – Reconstructions of the polystyrene sample (top) acquired on a Siemens X-ray source (20 kVp – 60 mA) and of an adult molar tooth at the Imaging beam line of the Brazillian synchrotron (polychromatic beam, mean energy: 19.9 keV). Left: no correction – Center: State of the art correction [5] – Right: pixel-by-pixel dead time correction.

POS(TIPP2014)212

## 4. Conclusion

We developed a new method for fast dead time calibration and pile-up correction. The experimental validation of dead time calibration was performed on a Medipix3RX ASIC bump bonded to 300- $\mu\text{m}$  Si sensor by comparing it with a standard method. The results on tomographic reconstructions show dramatic qualitative improvement compared to a state-of-the-art mathematical approach [5], enabling ring artefacts suppression without creating new artefacts. Furthermore, this new method presents the interest of enabling quantification of the reconstructed attenuation coefficients since it relies on a physical model of sinogram corruption. Further developments will focus on the limits of the method for higher dispersion, for example by expanding the Taylor approximation order. Finally, this method will be extended to other modalities of imaging, as phase contrast tomography and small angle scattering.

## References

- [1] P. Kraft, A. Bergamaschi, C. Bronnimann, R. Dinapoli, E.F. Eikenberry, H. Graafsma, B. Henrich, I. Johnson, M. Kobas, A. Mozzanica, C.M. Schlepütz, B. Schmitt, *Characterization and calibration of PILATUS detectors*, *IEEE Trans. Nucl. Sci. JHEP* **56** pp. 758–764, 2009
- [2] P. Pangaud, S. Basolo, N. Boudet, J.-F. Berar, B. Chantepie, J.-C. Clemens, P. Delpierre, B. Dinkespiler, K. Medjoubi, S. Hustache, M. Menouni, C. Morel, *XPAD3-S: A fast hybrid pixel readout chip for X-ray synchrotron facilities*, *Nucl. Instrum. Methods Phys. Res. A* **A591**, pp. 159–162, 2008
- [3] J. Rinkel, A. Brambilla, J.-M. Dinten, F. Mougél, *Method for correcting the stacking phenomenon applied to x-ray spectrums acquired using a spectrometric sensor*, *Patent WO2011064381 A1*, 2011
- [4] S. Titarenko, P. J. Withersb, A. Yagola, *An analytical formula for ring artefact suppression in X-ray tomography*, *Applied Math. Letter* **23**, pp.1489-1495, 2010
- [5] E.X. Miqueles, J. Rinkel, F. P. O'Dowd, J. S.V. Bermúdez, *Generalized Titarenko's Algorithm for Ring Artefacts Reduction* (accepted for publication in *Journal of Synchrotron Radiation* in 2014)
- [6] E.N. Gimenez, R. Ballabriga, M. Campbell, I. Horswell, X. Llopart, J. Marchal, K.J.S. Sawhney, N. Tartoni, D. Turecek, *Characterization of Medipix 3 with synchrotron radiation*, *IEEE Trans. Nucl. Sci.* **58**(1), pp. 323(10), 2011
- [7] Z. Vykydal, J. Jakubek, S. Pospisil, *USB interface for Medipix2 pixel device enabling energy and position-sensitive detection of heavy charged particles*, *Nucl. Instrum. Methods Phys. Res. A* **563**, pp. 112–115, 2006
- [8] K. Taguchi, M. Zhang, E.C. Frey, X. Wang, J.S. Iwaczy, E. Nygard, N.E. Hartsough, B.M. Tsui, W.C. Barber, *Modeling the performance of a photon counting x-ray detector for CT: Energy response and pulse pileup effects*, *Med Phys.* **38**(2), 1089–1102, 2011